Journal of Power Sources 195 (2010) 2969–2974

Contents lists available at ScienceDirect

Journal of Power Sources

journal homepage: www.elsevier.com/locate/jpowsour

Short communication

Battery algorithm verification and development using hardware-in-the-loop testing

Yongsheng He[a,*], Wei Liu[b], Brain J. Koch[b]

[a] General Motors Global Research and Development, 30500 Mound Road, MC 480-106-252, Warren, MI 48090, USA
[b] General Motors Global Vehicle Engineering, Warren, MI 48090, USA

ARTICLE INFO

Article history:
Received 25 September 2009
Received in revised form 6 November 2009
Accepted 9 November 2009
Available online 13 November 2009

Keywords:
Battery algorithm
Hardware-in-the-loop
State of charge
Power capability
Lithium-ion battery
Lithium iron phosphate battery

ABSTRACT

Battery algorithms play a vital role in hybrid electric vehicles (HEVs), plug-in hybrid electric vehicles (PHEVs), extended-range electric vehicles (EREVs), and electric vehicles (EVs). The energy management of hybrid and electric propulsion systems needs to rely on accurate information on the state of the battery in order to determine the optimal electric drive without abusing the battery.

In this study, a cell-level hardware-in-the-loop (HIL) system is used to verify and develop state of charge (SOC) and power capability predictions of embedded battery algorithms for various vehicle applications. Two different batteries were selected as representative examples to illustrate the battery algorithm verification and development procedure. One is a lithium-ion battery with a conventional metal oxide cathode, which is a power battery for HEV applications. The other is a lithium-ion battery with an iron phosphate ($LiFePO_4$) cathode, which is an energy battery for applications in PHEVs, EREVs, and EVs.

The battery cell HIL testing provided valuable data and critical guidance to evaluate the accuracy of the developed battery algorithms, to accelerate battery algorithm future development and improvement, and to reduce hybrid/electric vehicle system development time and costs.

1. Introduction

Hybrid electric vehicles (HEVs), plug-in hybrid electric vehicles (PHEVs), extended-range electric vehicles (EREVs), and electric vehicles (EVs) are emerging as important personal transportation options for petroleum displacement and energy diversification. Hybrid and electric propulsion systems offer superior well-to-wheel energy efficiency and significantly reduced vehicle emissions, particularly critical in this era of elevated demand for energy security and heightened concern over global warming.

The energy storage system is the key component and enabler to future hybrid and electric propulsion systems. Battery algorithms play a vital role in hybrid and electric vehicle applications, since the accuracy of battery algorithms have a significant impact on the energy efficiency and the battery's life. The energy management of hybrid and electric propulsion systems needs to rely on accurate information on the state of the battery (such as how much energy is left in the battery and how much power the battery can discharge or charge) in order to determine the optimal electric drive without abusing the battery.

Battery algorithms consist of state of charge (SOC) estimation, power capability prediction, and state of health (SOH) indication in general. The determination of SOC and power capability of a battery may be a problem of varying complexity depending on the battery type and on the application in which battery is used. When a battery algorithm is developed, it is necessary to test its accuracy, robustness, and other performance under real operating conditions. However, it is very challenging to test and verify the developed battery algorithm at the early development stage due to limited resources and time frame. In addition, usually the development vehicle may not be built and the energy management strategy may not be developed at this stage.

The hardware-in-the-loop (HIL) has been extensively used in the automotive industry for component development and rapid prototyping. Usually the target component in development is tested within a modeled system environment that reproduces the conditions under which the component will operate. With system-level requirements taken into consideration, HIL testing significantly reduces the time and costs of system-level integration and trouble-shooting later in the development cycle.

In this study, HIL testing is used to verify and develop battery algorithms for applications in hybrid electric vehicles (HEVs), plug-in hybrid electric vehicles (PHEVs), extended-range electric vehicles (EREVs), and electric vehicles (EVs). The focus of this study is to test and verify the embedded battery algorithms under the near real vehicle operating conditions. The battery HIL testing

* Corresponding author. Tel.: +1 586 9865679; fax: +1 586 9860176.
E-mail address: yongsheng.he@gm.com (Y. He).

0378-7753/$ – see front matter © 2009 Elsevier B.V. All rights reserved.
doi:10.1016/j.jpowsour.2009.11.036

provides valuable data and critical guidance to evaluate the accuracy of the developed battery algorithms and to accelerate battery algorithm future development and improvement. This will allow automotive manufacturers to accelerate hybrid/electric vehicle system overall development and to reduce hybrid/electric vehicle development costs.

2. Battery algorithms

Battery algorithms used in this study are greatly simplified battery equivalent circuit models, which have been shown to be one of effective ways to represent the battery system for vehicle applications [1–7]. Fig. 1(a) shows a reduced order model of a highly-distributed equivalent circuit, which consists of high-frequency ohmic resistance (R_{ohm}), charge transfer resistance (R_{ct}), double layer capacitance (C_{dl}), diffusion resistance (R_{diff}), and diffusion capacitance (C_{diff}).

As shown in Eq. (1), the terminal voltage (V) is a sum of open-circuit voltage V_{oc} (including thermodynamic voltage V_o and hysteresis voltage V_H), ohmic voltage ($V_{ohm} = I \cdot R_{ohm}$), double layer voltage (V_{dl}), and diffusion voltage (V_{diff}).

$$V = V_{oc} + I \cdot R_{ohm} + V_{dl} + V_{diff} \tag{1}$$

where V_{dl} and V_{diff} are determined from the following differential equations:

$$\frac{dV_{dl}}{dt} + \frac{1}{C_{dl} \cdot R_{ct}} V_{dl} = \frac{I}{C_{dl}} \tag{2}$$

$$\frac{dV_{diff}}{dt} + \frac{1}{C_{diff} \cdot R_{diff}} V_{diff} = \frac{I}{C_{diff}} \tag{3}$$

When the diffusion is ignored for some batteries such as the conventional lithium-ion battery, the battery equivalent circuit model is simplified to be a RC circuit without R_{diff} and C_{diff} as shown in Fig. 1(b). For other batteries such as the nickel metal hydride

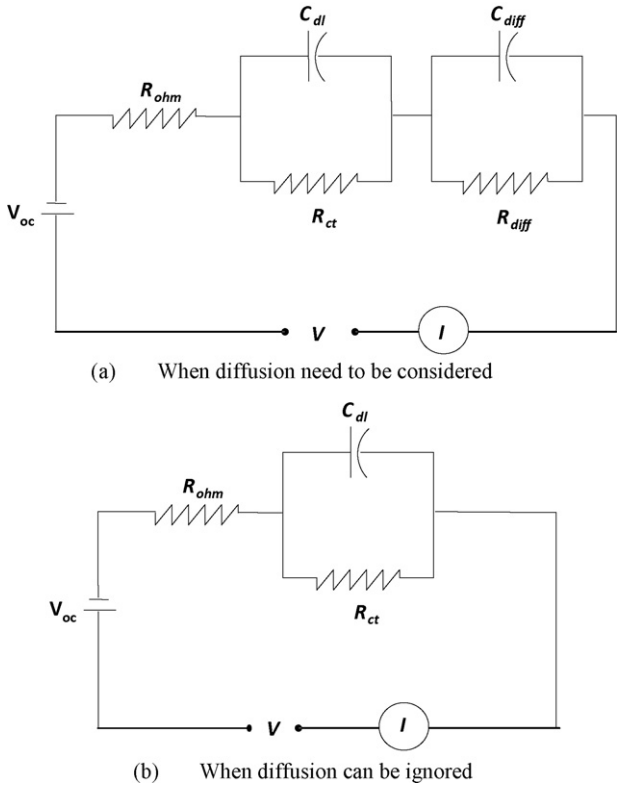

Fig. 1. Battery equivalent circuit models.

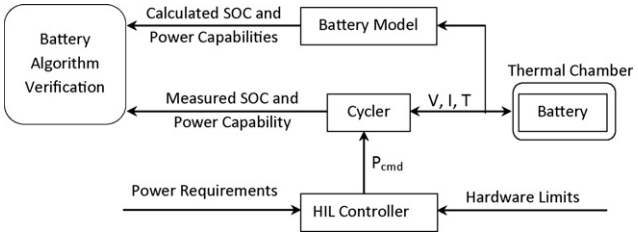

Fig. 2. Schematic of battery HIL testing setup and battery algorithm verification procedure.

(NiMH) battery and the lithium iron phosphate ($LiFePO_4$) lithium-ion battery, the diffusion is critical and need to be addressed. In this case, the battery equivalent circuit model with six parameters (V_{oc}, R_{ohm}, R_{ct}, C_{dl}, R_{diff}, C_{diff}) as illustrated in Fig. 1(a) can be used.

Using only quantities from previous and present time-steps, weighted recursive least-squares (WRLS) algorithm [4,5] was employed and proven highly effective to extract model parameters online. The hysteresis voltage V_H is not significant and could be ignored for lead-acid and conventional lithium-ion batteries. In the case of NiMH batteries, V_H must be taken into consideration and can be adaptively determined [5,6].

There are three important outputs from battery algorithms: state of charge (SOC), power capability, and state of health (SOH). This study focuses on the verification of SOC and power capability predictions of the battery algorithms.

SOC indicates the available energy stored in the battery. Generally, SOC can be estimated from current-based or voltage-based approaches. The current-based SOC (SOC_{Ah}) is estimated from the history of currents seen by the battery and calculated by coulomb integration. The voltage-based SOC (SOC_V) is directly correlated to the open-circuit voltage V_{oc} that is described by a modified Nernst equation [6].

For better predictive accuracy, a weighted sum of SOC_{Ah} and SOC_V was used in the battery algorithms, as shown in Eq. (4):

$$SOC = w \cdot SOC_{Ah} + (1 - w) \cdot SOC_V \tag{4}$$

where SOC_{Ah} is the stabilization signal, SOC_V is used as a correction signal, w is the weighting factor.

The power capability of a battery is how much power the battery can discharge or charge. The power capability can be approximated using the constant-voltage analytic solution [7], as given in Eq. (5):

$$P = \frac{V(V - V_0)}{R_{ohm} + R_{ct}} + V\left(\frac{V - V_{init}}{R_{ohm}} + I_{init} - \frac{V - V_0}{R_{ohm} + R_{ct}}\right) \times \exp\left[-\left(\frac{R_{ohm} + R_{ct}}{R_{ohm} R_{ct} C_{dl}}\right) \cdot t\right] \tag{5}$$

3. Battery HIL

Fig. 2 shows a general schematic of the setup for the battery HIL testing. The HIL system consists of a cycler, the battery (a cell, a module, or a pack) to be tested, a thermal chamber to control the temperature of the battery, and a HIL controller to coordinate commands and interactions of all components.

In this study, the cell-level HIL system is implemented and used in order to rapidly compare the performance of various battery cells and effectively evaluate the accuracy of battery algorithms, which are critical for component design very early in the development cycle. Compared with the pack-level HIL, the cell-level HIL is more effective to verify and develop battery algorithms because it avoids introducing pack-level complexity and system issues such as cell-to-cell variations and abuse concerns associated with the complete pack.

The battery cell is contained in a thermal chamber (Model 105A Test Equity) that has a controllable temperature range from −40 °C to 130 °C. The battery and the thermal chamber are connected to a cycler (Arbin Instruments, Model BT-2000) that can provide up to ±5 kW at 0.5–5 V. The cycler is controlled by a HIL controller that simulates the vehicle energy management system.

The major functions of the HIL controller include: transferring information and commands between the components (such as relaying power commands based on vehicle requirements), recording data (mainly cell voltages, currents, and temperatures), and overseeing battery performance parameters and their limits to avoid battery abuse.

The HIL system has the flexibility to use either a vehicle model to generate power requirements at different driving conditions, or vehicle-level signals taken from actual test vehicles. A more detailed illustration of the battery cell HIL setup using a vehicle model is provided elsewhere [8]. In this work, profiles of required powers from actual vehicles are taken and provided to the HIL controller as inputs, since they are more representative of on-road vehicle operations. The vehicle-level signals are processed and scaled for the cell-level HIL system.

The HIL controller has the option to command the required powers directly to the cycler within the hardware limits, or to adjust the required powers based on the allowable SOC usage window or practical power capability in order to test the battery under the near real vehicle operating conditions.

4. Battery algorithm verification procedure

In this study, the HIL bench is used extensively to verify the accuracy of battery algorithms, and a systematic approach is taken to formulate the verification procedure. Fig. 2 illustrates the procedure and schematic of the verification process.

First, the battery capability check test is run to check the capacity of the battery. After being properly initialized, the battery then runs through a profile of required powers (called a verification cycle profile) on the HIL bench.

At the end of the power profile, a SOC test or a charging (or discharging) power capability test is conducted. The SOC test is to measure how much the energy left in a battery by fully discharging it empty at 1 C rate (i.e., at a current that discharges the nominal capacity in 1 h) to its minimum operating voltage. The charging (or discharging) power test is to measure the maximum power of the battery by charging (or discharging) the battery to a pre-determined ceiling (or floor) voltage level. The ceiling (or floor) voltage is determined based on the maximum (or minimum) operating voltage along with the requirements to meet maximum current limits as in vehicle operations.

The battery model takes measured voltages, currents, and temperatures of the battery from HIL testing as inputs, and predicts the SOC and power capabilities over time. At the end of the verification cycle, the predictions of SOC and power capabilities are compared with those measured in the SOC test and the charging/discharging power tests. The power capabilities include the charging and discharging power capabilities instantaneously, 2 s, and 10 s after the verification cycle. Then the accuracy of the battery algorithm is assessed and reported.

5. Results and discussions

In this study, two different battery cells were tested on the HIL bench: one is a lithium-ion battery with a conventional metal oxide cathode; the other is a lithium-ion battery with an iron phosphate ($LiFePO_4$) cathode. The data from HIL testing were used to test and verify the embedded battery algorithms that can be implemented in hybrid electric vehicles (HEVs), plug-in hybrid electric vehicles (PHEVs), extended-range electric vehicles (EREVs), and electric vehicles (EVs). The two different batteries were selected as representative examples to illustrate the battery algorithm verification and development procedure. The lithium-ion battery is a power battery for HEV applications, while the $LiFePO_4$ lithium-ion battery is an energy battery for applications in PHEVs, EREVs, and EVs.

Table 1
Specifications of the conventional lithium-ion battery cell.

Nominal voltage (V)	3.6
Nominal capacity (Ah)	4.5
Nominal power (W)	500
Peak current (A)	200
Maximum operating voltage (V)	4.1
Minimum OPERATING Voltage (V)	2.7
Diameter (mm)	40
Length (mm)	92

5.1. Conventional lithium-ion battery

Table 1 lists the specifications of the conventional lithium-ion battery cell. It is a cylindrical cell with a nominal voltage of 3.6 V and a nominal capacity of 4.5 Ah.

A battery capacity check test was run first to check the capacity of the battery cell. The conventional lithium-ion battery cell sample has a checked capacity of 4.5 Ah.

To verify the accuracy of SOC and power capability predictions, a power profile recorded from an actual vehicle driven over the US Federal Test Procedure (FTP) cycle was used in the battery cell HIL. It is a charge-neutral power profile. Fig. 3 shows the conventional lithium-ion battery cell voltage, current, and power during the verification cycle. Note that there are three 500 W (nominal power) charging pulses and three 500 W discharging pulses in the cycle, which were added to verify the power capability predictions by the battery algorithm.

The conventional lithium-ion battery cell was tested on the HIL bench, the SOC and the power capabilities of the battery were

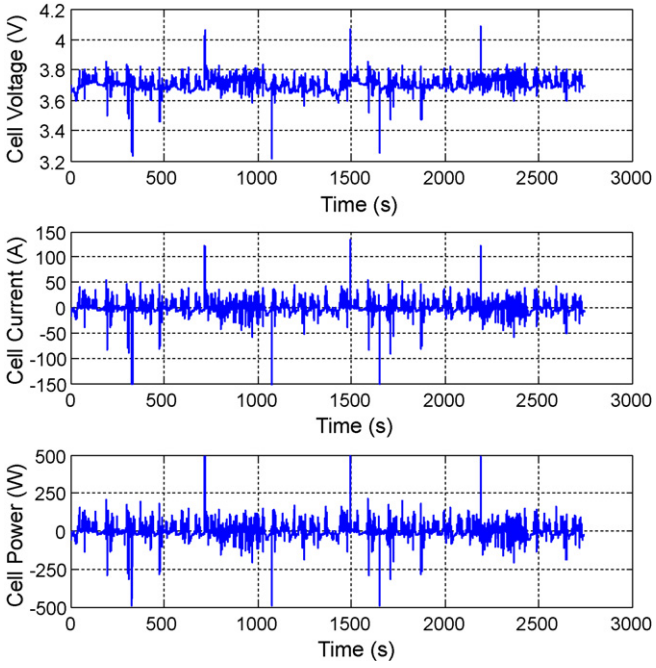

Fig. 3. Conventional lithium-ion battery cell voltage, current, and power profiles over the verification cycle.

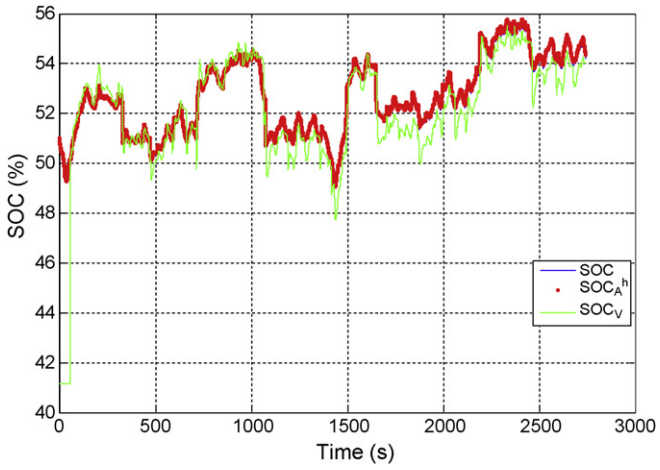

Fig. 4. Predicted SOC, SOC_{Ah}, and SOC_V of the conventional lithium-ion battery cell over the verification cycle.

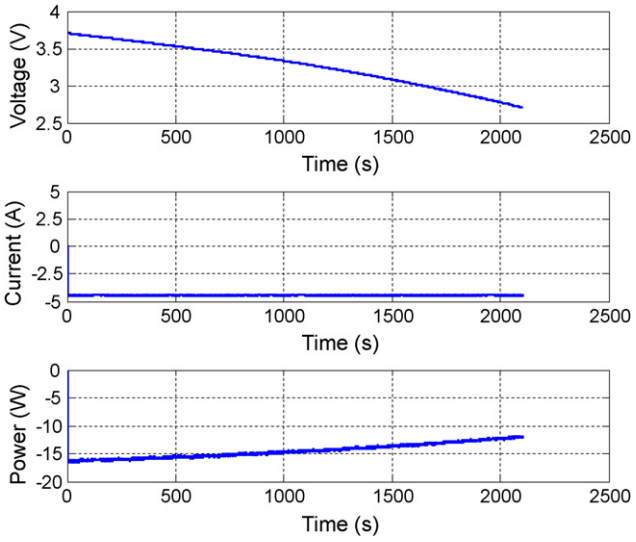

Fig. 5. Conventional lithium-ion battery cell voltage, current, and power measurements during the SOC test after the verification cycle.

assessed at various dynamic and static conditions for a HEV application, as discussed in the following sections.

5.1.1. SOC prediction verification

Fig. 4 shows the predicted SOC, SOC_{Ah}, and SOC_V of the conventional lithium-ion battery cell during the verification cycle. Note that the SOC_V signal quickly corrected from its initial value, and has very similar trend to that of SOC_{Ah}. It is also indicated that the weighting factor of SOC_V is relatively small in this case. As shown in Fig. 4, SOC signals are overlying very closely with SOC_{Ah}, which indicates the strong dependence of SOC predictions on SOC_{Ah}. At the end of the verification cycle, the SOC was predicted to be 54.3%.

To verify its accuracy, the battery cell was put to rest for 1 h after the verification cycle, and then a SOC test was conducted. The SOC test is basically to discharge the battery cell at 1 C rate until it is empty, and then the actual SOC and the error in SOC prediction are determined. Fig. 5 shows the conventional lithium-ion battery cell voltage, current, and power during the SOC test. By integrating the current over time, the measured SOC after the verification cycle was shown to be 58.4%.

5.1.2. Power capability prediction verification

During the verification cycle, the battery algorithm predicts the power capabilities of the conventional lithium-ion battery cell dynamically. Fig. 6 plots the charging and discharging power capabilities predicted by the lithium-ion battery algorithm, compared with the actual power measurements of the cell at 25 °C. As shown, the battery algorithm can predict 2 s and 10 s power capabilities reasonably well. The measured power pulses are bounded by the predicted 2 s and 10 s power capabilities, which indicates that the battery cell has sufficient power capabilities to provide the instantaneous power required over the whole cycle.

After the verification cycle, charging and discharging power tests were conducted to further verify the accuracy of power capability predictions. The voltage of the battery cell after the verification cycle was about 3.7 V. For the charging power test (see Fig. 7), the ceiling voltage was set to the maximum operating voltage 4.1 V and the power charged to the battery cell was measured. For the discharging power test (see Fig. 8), the floor voltage was set to 3.3 V to meet the maximum current limits and the power discharged

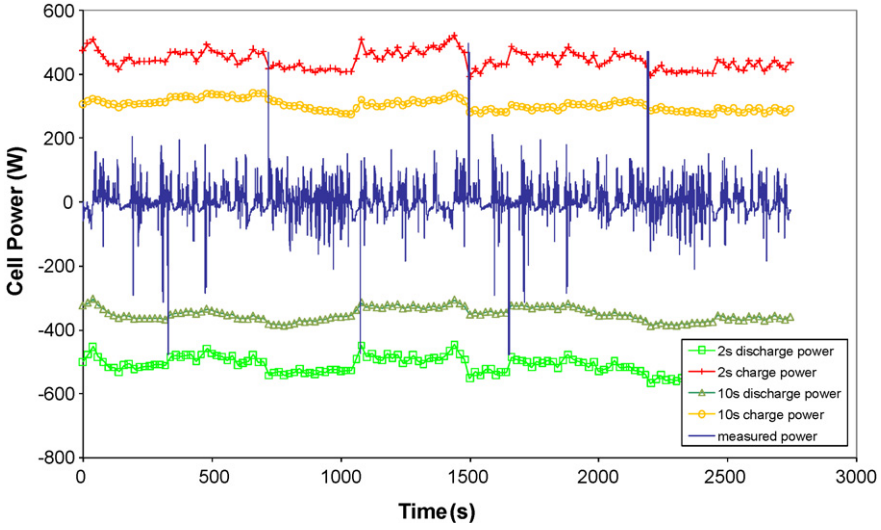

Fig. 6. Measured powers of the conventional lithium-ion battery cell during the verification cycle at 25 °C, compared with 2 s and 10 s charging and discharging power capabilities.

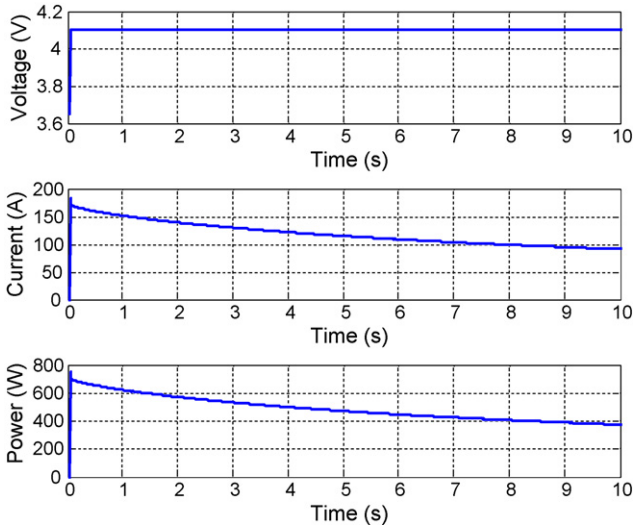

Fig. 7. Conventional lithium-ion battery cell voltage, current, and power measurements during the charging power test after the verification cycle.

was measured. The charging and discharging power tests lasted for 10 s. The power capability predictions instantaneously, 2 s, and 10 s after the verification cycle were recorded and compared with the measurements.

Fig. 9 demonstrates the accuracy of power capability predictions by the conventional lithium-ion battery algorithm after the verification cycle at 25 °C. The predicted instantaneous, 2 s, and 10 s charging powers agree very well with the measured charging power capabilities within 5% at 25 °C. It is observed that the discrepancy between predictions and measurements at 0.1 s is larger than that at 2 s and 10 s. It was attributed to the fact that there is always some overlap between regressed high-frequency ohmic resistance (R_{ohm}) and charge transfer resistance (R_{ct}) values. In other words, regressed R_{ohm} value contains some small fraction of R_{ct}. This is an artifact of the simplification that the battery equivalent circuit model makes of the electrochemical system, and also of the fact that the frequency of the input data waveforms is not always matched to the characteristic frequency of each parameter. As a result, for

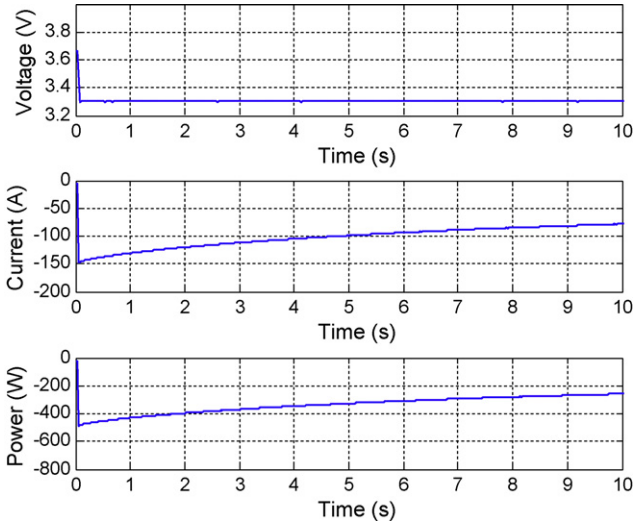

Fig. 8. Conventional lithium-ion battery cell voltage, current, and power measurements during the discharging power test after the verification cycle.

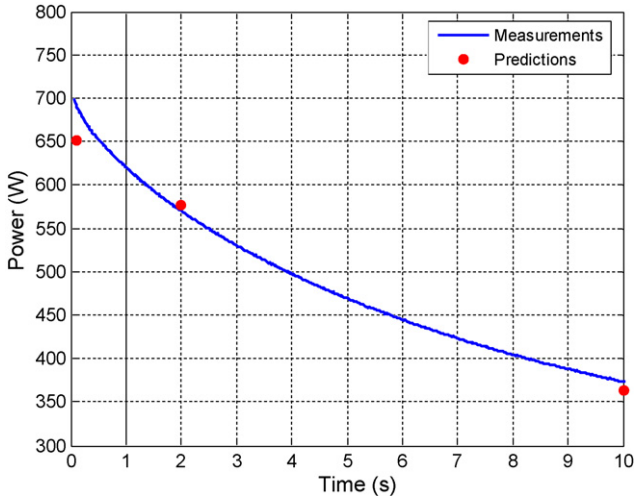

Fig. 9. Comparison between measured and predicted charging power capabilities by the conventional lithium-ion battery algorithm after the verification cycle.

Table 2
Specifications of the $LiFePO_4$ lithium-ion battery cell.

Nominal voltage (V)	3.3
Nominal capacity (Ah)	15
Peak current (A)	250
Maximum operating voltage (V)	3.6
Minimum operating voltage (V)	2.0
Thickness (mm)	7.5
Width (mm)	150
Length (mm)	202

short power pulses whose behavior should be dominated by R_{ohm}, the slight overlap of R_{ohm} and R_{ct} causes the power to be underpredicted. For longer power pulses, R_{ct} makes a major contribution and the overlap is less important, and hence the model has a better predictive accuracy.

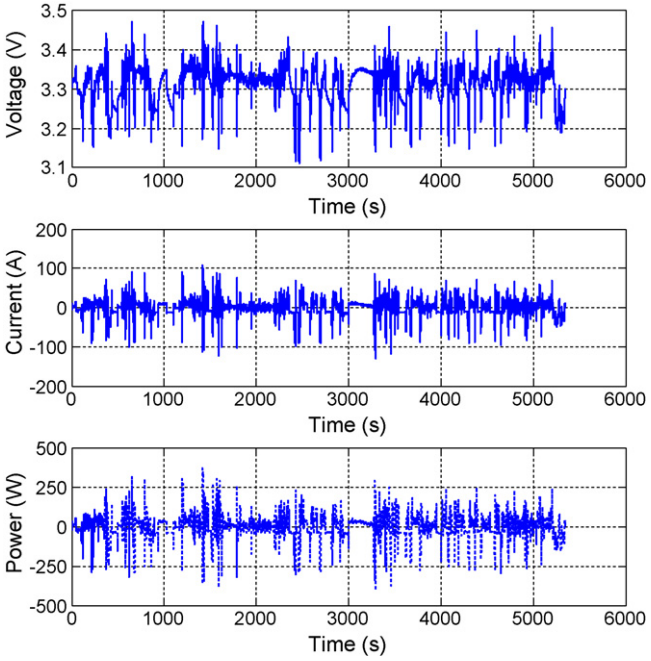

Fig. 10. $LiFePO_4$ lithium-ion battery cell voltage, current, and power measurements during the verification cycle.

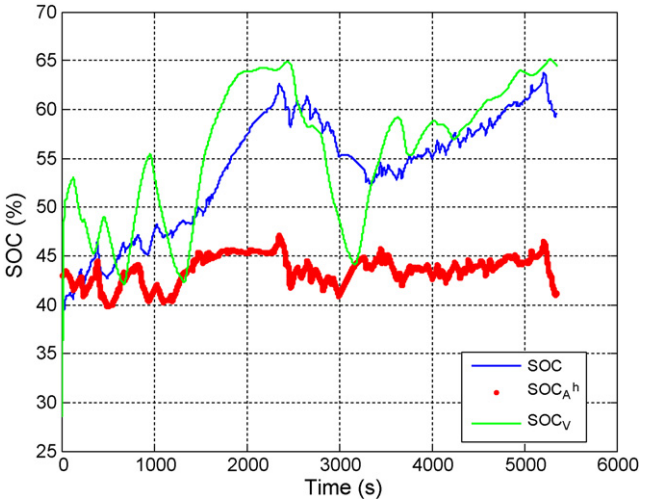

Fig. 11. Predicted SOC, SOC_{Ah}, and SOC_V of the $LiFePO_4$ lithium-ion battery cell over the verification cycle.

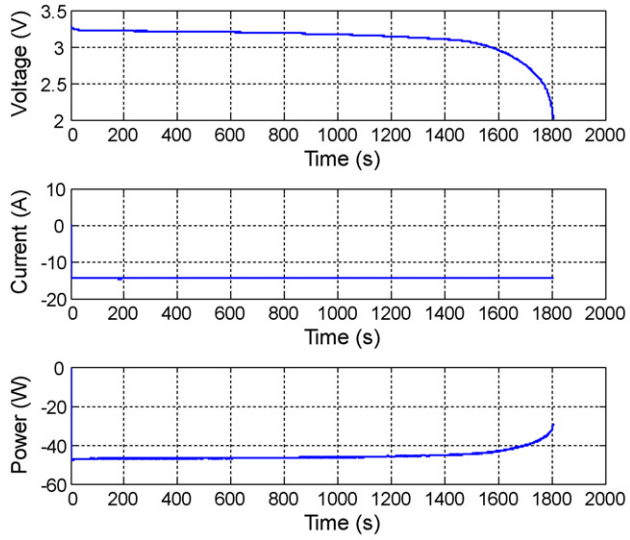

Fig. 12. $LiFePO_4$ lithium-ion battery cell voltage, current, and power measurements during the SOC test after the verification cycle.

5.2. *$LiFePO_4$ lithium-ion battery*

The second battery cell that was tested on HIL bench was a $LiFePO_4$ lithium-ion battery cell, and its specifications are listed in Table 2. It is a prismatic cell with a nominal voltage of 3.3 V and a nominal capacity of 15 Ah. This study presents only the validation of SOC prediction of the battery algorithm for the $LiFePO_4$ lithium-ion battery, while the power capability prediction is still under development.

First the capacity of the battery cell was checked. The $LiFePO_4$ lithium-ion battery cell sample has a checked capacity of 14.05 Ah.

Fig. 10 shows the verification test cycle that was taken from another development vehicle for the $LiFePO_4$ lithium-ion battery cell. Fig. 11 compares the SOC, SOC_{Ah}, and SOC_V predicted by the $LiFePO_4$ lithium-ion battery algorithm over the verification cycle. As shown, the weighting of SOC_V was significant. The SOC after the verification cycle was predicted to be 59.6%. Note that the initial SOC of the battery model at the beginning of the verification cycle was set to 43% on purpose, while the battery cell tested in HIL started with an initial SOC of 50%. The initial value for SOC was set to 43% in order to verify the accuracy of the battery algorithm at randomly selected initial conditions and how well the battery algorithm may correct from an incorrect SOC initial value adaptively.

After the verification cycle, a SOC test was conducted to verify the accuracy of the SOC prediction. Fig. 12 illustrates the voltage, current, and power measurements during the SOC test. The measured SOC after the verification cycle was 50.2%. The discrepancy between the measured and predicted SOC is attributed to a larger error in SOC_V that is primarily caused by the characteristics of a flat open-circuit voltage V_{oc} over a wide range of SOC as well as hysteresis for the $LiFePO_4$ lithium-ion battery.

6. Conclusions

A battery cell-level HIL system was implemented and employed to validate and develop the battery algorithms for a conventional lithium-ion battery and a $LiFePO_4$ lithium-ion battery. A systematic verification procedure was formulated to verify the accuracy of SOC and power capability predictions of various battery algorithms.

The SOC predictions of the conventional lithium-ion battery algorithm were verified with a charge-neutral power profile recorded from an actual vehicle driven over the FTP cycle. At the end of the verification cycle, the SOC was predicted to be 54.3%, compared with the measurement of 58.4%. The tested power capabilities of the conventional lithium-ion battery include the instantaneous, short-term, and long-term charging/discharging power capabilities at 25 °C. The power capability predictions of the battery algorithm are reasonable; the predicted instantaneous, 2 s and 10 s charging power capabilities agree very well with the measurements within 5%.

The SOC predictions of the $LiFePO_4$ lithium-ion battery algorithm were verified with a power profile recorded from an actual vehicle driven over a different verification cycle. At the end of the verification cycle, the SOC was predicted to be 59.6%, compared with the measurement of 50.2%.

The HIL testing data provided critical guidance for further development and improvement of the battery algorithms, especially their power capability predictions. This accelerates overall system development process and reduces the cost of the hybrid/electric vehicle development.

Acknowledgements

The author would like to acknowledge Damon Frisch, Jian Lin, Rezina Nabi, and John Novak for their strong support and helpful discussions.

References

[1] J.M. Miller, Propulsion Systems for Hybrid Vehicles, Institution of Electrical Engineering and Technology, London, UK, 2004.
[2] A.J. Bard, L.R. Faulkner, Electrochemical Methods: Fundamentals and Applications, Wiley, New York, USA, 1980.
[3] I.J. Ong, J. Newman, J. Electrochem. Soc. 146 (12) (1999) 4360–4365.
[4] M.W. Verbrugge, D. Frisch, B.J. Koch, J. Electrochem. Soc. 152 (2005) A333–A342.
[5] M.W. Verbrugge, B.J. Koch, J. Electrochem. Soc. 153 (2006) A187–A201.
[6] M.W. Verbrugge, E.D. Tate, J. Power Sources 126 (2004) 236–249.
[7] M.W. Verbrugge, in: M. Schlesinger (Ed.), Modern Aspects of Electrochemistry, Modeling and Numerical Simulations I, vol. 43, Springer, New York, 2009.
[8] C. Massey, A. Bekaryan, P. Liu, A. Parulian, L. Turner, D. Frisch, T. Weber, M. Verbrugge, Hardware-in-the-loop testing for electrochemical cells in hybrid electric vehicles, SAE paper 2005-01-3500, 2005.